# DOUBLE-SIDED ULTRASONIC TESTING AND IMAGING OF MULTILAYER COMPOSITES WITH OUT-OF-PLANE FIBER WRINKLING

## MENGLONG LIU [1] AND ZHUANG LI [1]

[1]School of Mechanical Engineering and Automation, Harbin Institute of Technology, Shenzhen 518055, P.R. China
liumenglong@hit.edu.cn

**Keywords:** Fiber reinforced polymer laminates, Ultrasonic testing, Out-of-plane fiber wrinkling, Finite Element Analysis

**Abstract.** For fiber reinforced polymers (FRPs), ply stacking errors and fiber waviness during manufacturing will have a great influence on the mechanical properties of composites, which requires non-destructive testing and evaluation (NDT&E) for potential structure defects. Herein, this study analyzes the ultrasonic echo signals in pulse-echo (PE) mode to assess the layered structure and sub-structure of laminates, analytically and numerically. Based on recursive stiffness matrix method and analytic-signal technology, analytical modeling is performed to investigate the propagation of ultrasound and detect the layered structure in flat laminates. In addition, a numerical finite element model is built to further study the propagation of ultrasound in wavy composites. Based on the circular variances of ply angles extracted by structure tensor analysis, the double-sided ultrasonic testing and B-scan imaging method is proposed to correct the imaging artifact areas of wavy composites. After statistical validation, this weighted sum method can indeed reduce the influence of ultrasonic beam deviation caused by out-of-plane fiber wrinkling, thereby improving the imaging effect in wavy composites.

## 1. INTRODUCTION

FRPs are the most widely used composites nowadays, which feature the high strength of fiber and the good machinability of matrix. Among many lightweight materials, FRP has high specific strength and specific stiffness, and is widely used in aerospace, military, and construction fields. FRP is manufactured by stacking layer by layer. During the process of stacking, composites, especially those with complex shapes, may deviate from the expected structure, like the out-of-plane fiber wrinkling in the thickness direction. These layered structure and sub-structure will play an important role in the mechanical properties of composites including tensile, compression and fatigue strength [1]. In order to reduce potential failures, it is necessary to detect and characterize the internal features and defects of composites without destroying the original structure through non-destructive testing and evaluation (NDT&E) methods.

Of all the NDT&E methods, the advantages of ultrasonic testing (UT) include convenient operation, fast scanning speed, high resolution, and *in-situ* detection. Although UT has been widely used to detect defects such as delamination or porosity, the measurement of fiber

waviness remains a technical challenge because of ultrasonic beam deviation and the difference of flight time [2]. Therefore, it is necessary to study the propagation of ultrasound in laminates firstly. Rokhlin et al. [3] proposed the recursive stiffness matrix method to obtain the reflection waveform. Following Rokhlin's research, R. A. Smith et al. [4] reconstructed the internal ply structure of laminates using the instantaneous phase based on analytic-signal technology. X. Yang et al. [5] further studied the influence of several key parameters on tracking resin interplies.

Analytical model is easy to calculate and flexible in parameter changes, but it's only suitable for the flat and alternating "fiber ply-resin interply" laminates model to study the interlayer interface and single A-scan signal. Instead, it cannot characterize complex internal features like fiber waviness, so numerical modeling and finite element analysis (FEA) are required. Z. Zhang et al. [6] used OnScale® to build a FRP laminates model with defects including delamination, local rich resin, and out-of-plane fiber wrinkling. Meanwhile, they studied the frequency dependence of echo signals corresponding to delamination and local rich resin. However, they did not pay too much attention to the reconstruction and imaging of layered structure and out-of-plane wrinkling.

After getting the imaging results, the methods for evaluating the local orientation of an image include matched-filter methods, image-transform methods, and gradient methods. L.J. Nelson et al. [7] used the structure tensor image processing method which belonged to gradient methods, to evaluate the ply orientations and extract the ply angles of FRP laminates. However, the imaging effect of deep plies was relatively poor, and there was no clear evaluation index for the extracted ply angles. Moreover, the sample had a ply spacing of 189 μm and a resin interply thickness of 40 μm, which deviated from the actual situation.

In this study, we analyze the ultrasonic echo signals of resin interplies to assess the layered structure and sub-structure of laminates, analytically and numerically. Section 2 describes the analytical modeling of the propagation of ultrasound in flat FRP laminates. Based on the numerical model, the double-sided ultrasonic imaging method of FRP laminates with out-of-plane fiber wrinkling is proposed to correct artifact areas in Section 3. In the end, concluding remarks are presented in Section 4.

## 2. ANALYTICAL MODELING

### 2.1 Modeling setup

In this study, our research object is a 32-layer unidirectional FRP laminates. The ply spacing $l$ is 125 μm, which is composed of 115 μm fiber ply and 10 μm resin interply. The input signal is a Gaussian modulated pulse. According to the ply resonance theory, the response signal amplitude is maximized when the frequency of excitation pulse coincides with the resonance frequency of composite layer. The longitudinal wave velocity of composite layer $c$ is 2630 m/s, and the fundamental resonance frequency $f_1$ is

$$f_1 = \frac{nc}{2l} = \frac{1 \times 2630}{2 \times 125} = 10.52 \, \text{MHz} . \tag{1}$$

Therefore, the center frequency $F_c$ is set as 10 MHz, and the fractional bandwidth $W$ is 0.8.

Recursive stiffness matrix method relates the top-layer and bottom-layer of FRP laminates by recursively solving the stiffness matrix of layers. And the total stiffness matrix **K** of FRP is

$$\begin{bmatrix} \boldsymbol{\sigma}_0 \\ \boldsymbol{\sigma}_N \end{bmatrix} = \begin{bmatrix} \mathbf{K}_{11} & \mathbf{K}_{12} \\ \mathbf{K}_{21} & \mathbf{K}_{11} \end{bmatrix} \begin{bmatrix} \mathbf{u}_0 \\ \mathbf{u}_N \end{bmatrix}, \tag{2}$$

where $(\boldsymbol{\sigma}_0, \mathbf{u}_0)$ and $(\boldsymbol{\sigma}_N, \mathbf{u}_N)$ are the stress and displacement vector of the upper-surface and lower-surface of FRP laminates, respectively.
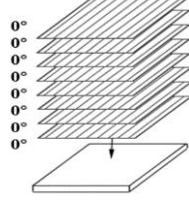


Figure 1: Structure of unidirectional composite laminates.

## 2.2   Results analysis

The reflection coefficient $R$ of acoustic wave can then be obtained with the recursive stiffness matrix method, and the echo signal is shown in Figure 2 (a). Analytic signal $s_a(t)$ is a complex function whose real part $s(t)$ and imaginary part $g(t)$ are associated by Hilbert transform,

$$s_a(t) = s(t) + ig(t) = A_{inst}(t)e^{i\Phi_{inst}(t)}, \tag{3}$$

where $A_{inst}(t)$ and $\Phi_{inst}(t)$ are the instantaneous amplitude and phase respectively.

The instantaneous phase of the echo signal and corresponding B-scans are shown in Figure 2 (b) and (c-d) respectively, from which we can track 32 layers. Compared with amplitude, instantaneous phase is less affected by depth and attenuation, and more resistant to interference.
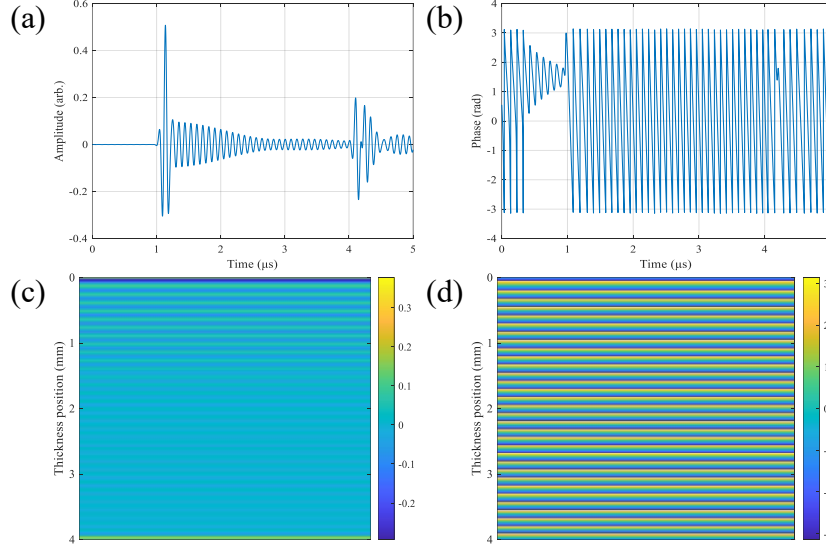


Figure 2: Response signal. (a) magnitude, (b) phase, (c) magnitude B-scan, (d) phase B-scan.

## 3.  NUMERICAL MODELING

### 3.1   FEA setup

The mesh of unidirectional FRP laminates is generated in MATLAB®, and layers are

constructed by continuous curves to simulate the out-of-plane fiber wrinkling, as shown in Figure 3 (a). The ply spacing $l$ is 125 μm, which is composed of 115 μm fiber ply and 10 μm resin interply. The coordinates $z$ in the thickness direction and the ply angle $\alpha$ at each point are

$$z = z_0 - A\left(\frac{1}{2} + \frac{1}{2}\cos\left(\frac{2\pi(u_z - z_0)}{\lambda_z}\right)\right)\sin\left(\frac{2\pi x}{\lambda_x}\right),\tag{4}$$

$$\alpha = \arctan\left(\frac{dz}{dx}\right) = \arctan\left(-\frac{2\pi A}{\lambda_x}\left(\frac{1}{2} + \frac{1}{2}\cos\left(\frac{2\pi(u_z - z_0)}{\lambda_z}\right)\right)\cos\left(\frac{2\pi x}{\lambda_x}\right)\right).\tag{5}$$

where $z_0$ is the coordinate when there is no fiber wrinkling in $z$-direction, $\lambda_z$ is the thickness of the fiber wrinkling area, $u_z$ is the coordinate of the center of fiber wrinkling area in $z$-direction, $\lambda_x$ is the wavelength of fiber wrinkling in $x$-direction, and $A$ is the magnitude of fiber wrinkling. The parameter values of $s$ of FRP laminates are shown in Table 1, where $tkn$ is the total thickness of FRP laminates, and $\alpha_{max}$ is the maximum ply angle $\alpha$.

**Table 1**: Geometry parameters of FRP laminates with fiber wrinkling.

| Parameter | $\lambda_x$ (mm) | $\lambda_z$ (mm) | $u_z$ (mm) | $tkn$ (mm) | $l$ (μm) | $A$ (mm) | $\alpha_{max}$ (°) |
|---|---|---|---|---|---|---|---|
| Value | 15 | 4 | 2 | 4 | 125 | 0.5 | 12 |

The mesh generated in MATLAB® is imported into OnScale® as Figure 3 (b). The top and bottom of the FRP laminates are covered with water. A row of planar probes is placed on both sides, but only one side of probes is used at a time. The probes on this side are excited at the same time but receive signals respectively, and the excitation center frequency is 10 MHz.
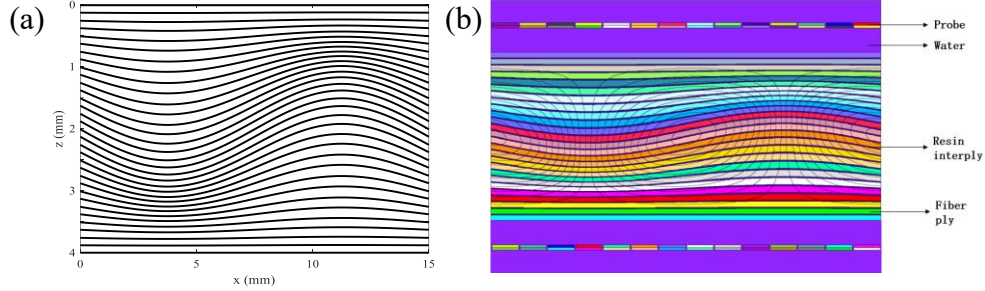


**Figure 3**: FRP laminates model with fiber wrinkling in (a) MATLAB® and (b) OnScale®.

The mesh in $x$- and $z$-direction of the whole model is 20 μm and 10 μm, respectively. A benchmark study is then carried out on the mesh size in $z$-direction of FRP laminates $z_2$. When $z_2$ is set as 1/3 of the resin interply thickness, namely, 10/3 μm, the response signal is basically close to that of mesh $z_2 = 10/5$ μm as Figure 4, and can strike a balance between accuracy and computational resource.
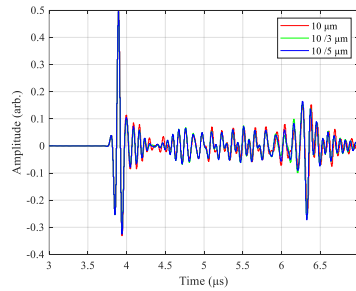


**Figure 4**: Comparison of response signals of different mesh sizes.

4

## 3.2 Signal processing

Figure 5 (a-b) show the time and frequency domains of the original response signal at $x = 7.5$ mm. (c-d) are the B-scans obtained from the original response signal. Since the simulation settings are ideal and almost noiseless, signal filtering is not required.
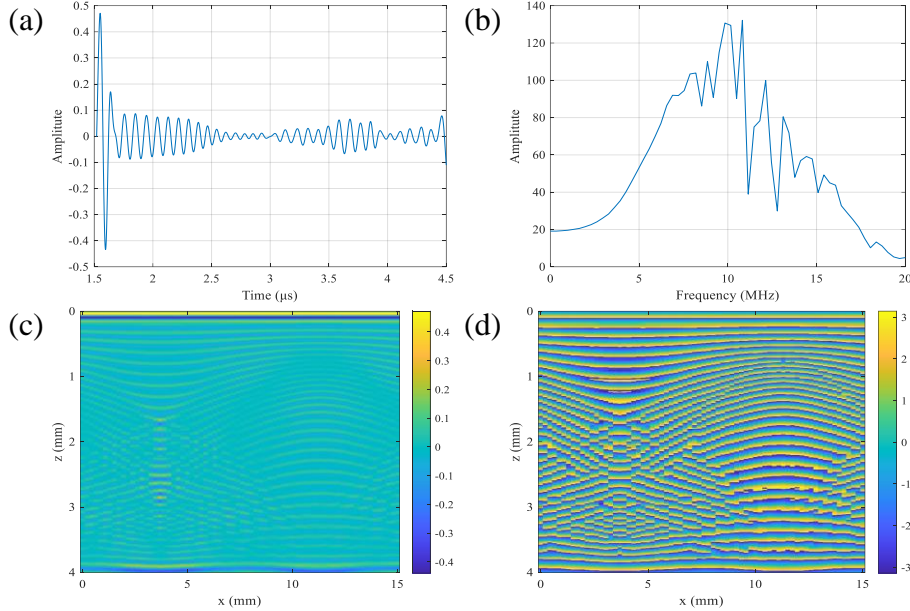


**Figure 5**: Original response signal. (a) Time domain and (b) frequency domain of response signal at $x = 7.5$ mm; (c) magnitude B-scan, (d) phase B-scan.

Due to the limited number of probes, there are some discontinuous step-like shapes in the original phase B-scan Figure 5 (d). Therefore, the data in $x$-direction is interpolated 10 times to improve the resolution in the horizontal direction of image. In addition, the time step in $z$-direction is too small because of small mesh $z_2$. Consequently, the sample frequency is so large that there is too much time-domain signal data. Herein, time-domain signal is extracted as 1/10 of the original signal, ensuring the amount of data in $x$- and $z$-direction is in the same order of magnitude. B-scan then becomes continuous as Figure 6, which is suitable for image processing.
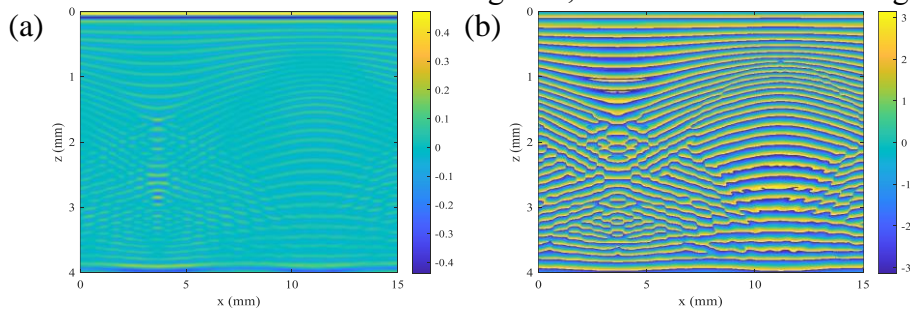


**Figure 6**: (a) Magnitude B-scan and (b) phase B-scan after interpolation in x-direction and extraction in z-direction.

## 3.3 Image processing

Structure tensor $\mathbf{T}(\mathbf{p})$ can obtain the orientation information by calculating the local average of the outer product of the gradients in a specified neighborhood $\mathbf{x}$ around pixel $\mathbf{p}$,

$$\mathbf{T}(\mathbf{p}) = \int G_\tau(\mathbf{x}) \left[ \nabla I \right](\mathbf{x}) \left[ \nabla^\mathrm{T} I \right](\mathbf{x}) d\mathbf{x} \,, \tag{6}$$

where $G_\tau(\mathbf{x})$ is a Gaussian window function with standard deviation $\tau$, and $\nabla I$ is the gradient vector of the image intensity $I$ at pixel $\mathbf{p}$. To smooth $\nabla I$, $I$ is convolved with another Gaussian window function $G_\sigma(\mathbf{x})$ with standard deviation $\sigma$ to obtain $\nabla_\sigma I$ before getting the gradient. $\tau$ and $\sigma$ are called integration scale and noise scale, which are set as 0.3 and 5 respectively. The magnitude of them will have an influence on the magnitude of extracted ply angle $\alpha$.

For phase B-scans of single-side excitation models, the ply angles $\alpha$ of pixels are extracted using structure tensor, as shown in Figure 7 and Figure 8.
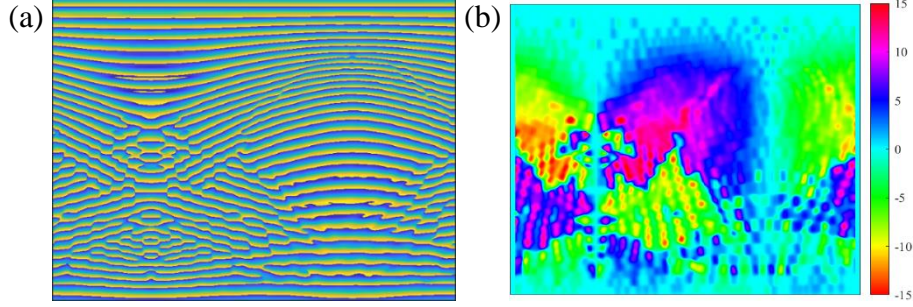


**Figure 7**: (a) Phase B-scan and (b) ply angle $\alpha$ of upper-side excitation model.
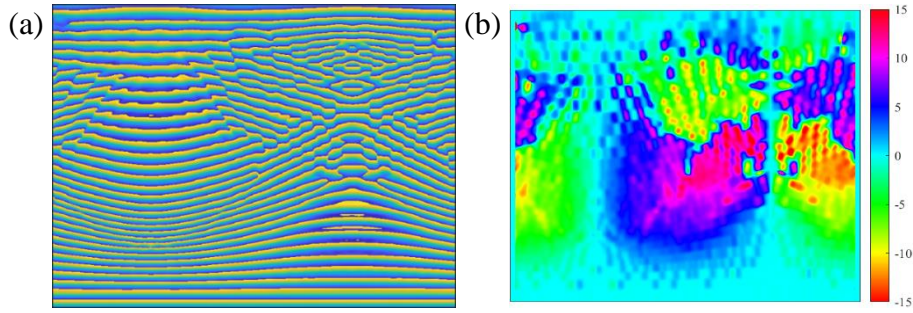


**Figure 8**: (a) Phase B-scan and (b) ply angle $\alpha$ of lower-side excitation model.

Then Phase B-scans are divided into several patches according to the image size and angle distribution, and the circular variances of ply angles of patches are calculated. The phase of the weighted sum model is obtained by weighting the phase of the upper-side and lower-side excitation model using the inverse of circular variances of corresponding patches. And then the ply angles $\alpha$ of weighted sum model can be extracted using structure tensor as Figure 9.
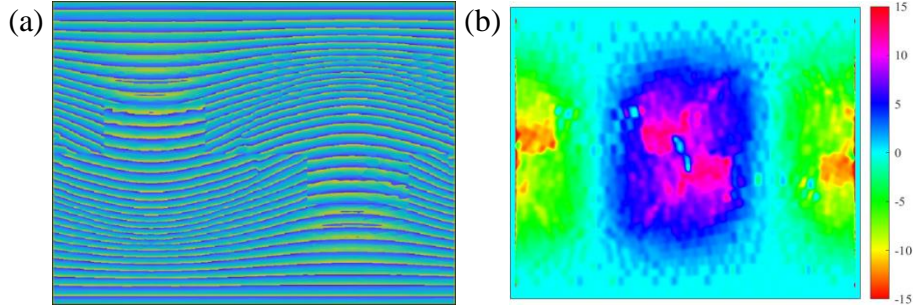


**Figure 9**: (a) Phase B-scan and (b) ply angle $\alpha$ of weighted sum model.

6

Figure 7 to Figure 10 are images of the upper-side excitation, lower-side excitation, weighted sum, and reference standard model, respectively. (a) is the phase B-scan, and (b) is the distribution of ply angle $\alpha$ at each pixel of the image. It can be seen that in the left-down part of Figure 7 and the right-up part of Figure 8, there are imaging artifact areas which are significantly different from Figure 10 due to ultrasonic beam deviation and the difference of flight time. And Figure 9 corrects these artifact areas to a certain extent.
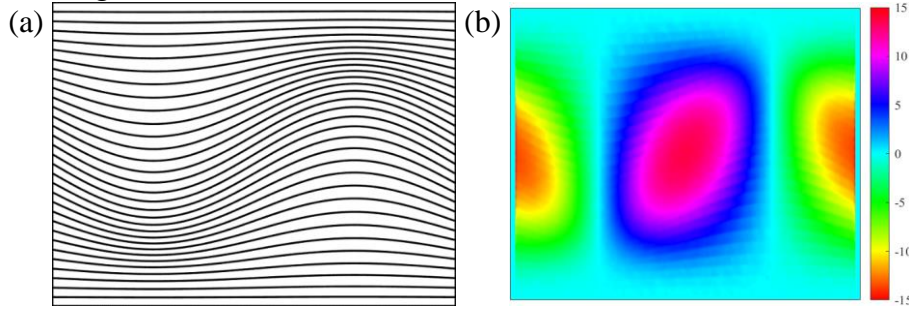


**Figure 10**: (a) Phase B-scan and (b) ply angle $\alpha$ of reference standard model.

## 3.4  **Statistical analysis**

To illustrate the validity of the above weighted sum method, statistical analysis is performed. In linear statistics, the Pearson correlation coefficient $\rho_{X, Y}$ is used to measure the linear correlation between two variables $X$ and $Y$. And in circular statistics [8] which is more suitable for analyzing directional data like angle, circular correlation between two directional variables can be assessed by computing the circular-circular correlation coefficient $\rho_{cc}$,

$$\rho_{cc} = \frac{\sum_i \sin(\alpha_i - \bar{\alpha})\sin(\beta_i - \bar{\beta})}{\sqrt{\sum_i \sin^2(\alpha_i - \bar{\alpha})\sin^2(\beta_i - \bar{\beta})}} \,, \tag{7}$$

where $\bar{\alpha}$ and $\bar{\beta}$ are the sample mean directions.

Table 2 shows the correlation coefficients of ply angle $\alpha$ between models and reference standard model. Both $\rho_{X, Y}$ and $\rho_{cc}$ indicate that weighted sum model is significantly better than the single-side excitation models, proving the validity of weighted sum method from the perspective of ply angle data.

**Table 2**: Correlation coefficients of ply angle $\alpha$ between models and reference standard model Figure 10.

| Model | Upper-side excitation | Lower-side excitation | Weighted sum |
|---|---|---|---|
| $\rho_{X, Y}$ | 0.7040 | 0.6952 | 0.8116 |
| $\rho_{cc}$ | 0.3932 | 0.3785 | 0.6206 |

## 4.  **CONCLUDING REMARKS**

In this study, we study the propagation of ultrasound in flat and wavy composites to assess the layered structure and sub-structure of FRP laminates. The double-sided ultrasonic testing and B-scan imaging method is proposed to improve the imaging effect in wavy composites. A unidirectional FRP laminates model is built with a ply spacing of 125 μm and a resin interply thickness of 10 μm, which is more in line with the reality but will bring challenges because 10

μm is so thin that the amplitude of echo signal will be very small. And it turns out that there are some imaging artifact areas in wavy regions due to ultrasonic beam deviation and the difference of flight time. Then the proposed weighted sum method corrects these artifact areas based on the circular variances of ply angles. What's more, correlation coefficients between models and reference standard model prove the validity of this method from a statistical point of view. The experimental study will be carried out in the future.

## REFERENCES

[1] P. Kulkarni, K.D. Mali, S. Singh, An overview of the formation of fibre waviness and its effect on the mechanical performance of fibre reinforced polymer composites, Compos. Part A Appl. Sci. Manuf. 137 (2020) 106013. https://doi.org/10.1016/j.compositesa.2020.106013.

[2] Z. Zhang, Q. Li, M. Liu, W. Yang, Y. Ang, Through transmission ultrasonic inspection of fiber waviness for thickness-tapered composites using ultrasound non-reciprocity: Simulation and experiment, Ultrasonics. 123 (2022) 106716. https://doi.org/10.1016/j.ultras.2022.106716.

[3] S.I. Rokhlin, L. Wang, Stable recursive algorithm for elastic wave propagation in layered anisotropic media: Stiffness matrix method, J. Acoust. Soc. Am. 112 (2002) 822–834. https://doi.org/10.1121/1.1497365.

[4] R.A. Smith, L.J. Nelson, M.J. Mienczakowski, P.D. Wilcox, Ultrasonic Analytic-Signal Responses from Polymer-Matrix Composite Laminates, IEEE Trans. Ultrason. Ferroelectr. Freq. Control. 65 (2018) 231–243. https://doi.org/10.1109/TUFFC.2017.2774776.

[5] X. Yang, E. Verboven, B. feng Ju, M. Kersemans, Parametric study on interply tracking in multilayer composites by analytic-signal technology, Ultrasonics. 111 (2021) 106315. https://doi.org/10.1016/j.ultras.2020.106315.

[6] Z. Zhang, S. Guo, Q. Li, F. Cui, A.A. Malcolm, Z. Su, M. Liu, Ultrasonic detection and characterization of delamination and rich resin in thick composites with waviness, Compos. Sci. Technol. 189 (2020) 108016. https://doi.org/10.1016/j.compscitech.2020.108016.

[7] L.J. Nelson, R.A. Smith, M. Mienczakowski, Ply-orientation measurements in composites using structure-tensor analysis of volumetric ultrasonic data, Compos. Part A Appl. Sci. Manuf. 104 (2018) 108–119. https://doi.org/10.1016/j.compositesa.2017.10.027.

[8] P. Berens, CircStat : A MATLAB Toolbox for Circular Statistics, J. Stat. Softw. 31 (2009). https://doi.org/10.18637/jss.v031.i10.